Biosensors and Bioelectronics 126 (2019) 624–631

Contents lists available at ScienceDirect

Biosensors and Bioelectronics

journal homepage: www.elsevier.com/locate/bios

Comprehensive human stem cell differentiation in a 2D and 3D mode to cardiomyocytes for long-term cultivation and multiparametric monitoring on a multimodal microelectrode array setup

Stephan Fleischer[a], Heinz-Georg Jahnke[a], Enrico Fritsche[a], Mathilde Girard[b], Andrea A. Robitzki[a,*]

[a] Centre for Biotechnology and Biomedicine, Universität Leipzig, Division of Molecular Biological-Biochemical Processing Technology, Germany
[b] CECS, I-STEM Paris, AFM, Institute for Stem cell Therapy and Exploration of Monogenic Diseases, France

ARTICLE INFO

Keywords:
Induced pluripotent stem cell derived human cardiomyocytes
Multiparametric bioelectronic maturation monitoring
Accelerated cardiac maturation
3D cultures

ABSTRACT

Human pluripotent stem cell derived cardiomyocytes are a promising cell source for research and clinical applications like investigation of cardiomyopathies and therefore, identification and testing of novel therapeutics as well as for cell based therapy approaches. However, actually it´s a challenge to generate matured adult cardiomyocyte-like phenotype in a reasonable time. Moreover, there is a lack of applicable non-invasive label-free monitoring techniques providing quantitative parameters for analysing the culture stability and maturation status. In this context, we established an efficient protocol based on a combined differentiation of hiPSC in 2D cultures followed by a forced reaggregation step that leads to highly enriched (> 90% cardiomyocytes) cardiomyocyte clusters. Interestingly, 3D cultures revealed an accelerated maturation as well as phenotype switch from atrial to ventricular cardiomyocytes. More strikingly using combined impedimetric and electrophysiological monitoring the high functionality and long-term stability of 3D cardiomyocyte cultures, especially in comparison to 2D cultures could be demonstrated. Additionally, chronotropic as well as QT-prolongation causing reference compounds were used for validating the cardio specific and sensitive reaction over the monitored time range of more than 100 days. Thus, the approach of multiparametric bioelectronic monitoring offers capabilities for the long-term quantitative analysis of hiPS derived cardiomyocyte culture functionality and long-term stability. Moreover, the same multiparametric bioelectronic platform can be used in combination with validated long-term stable cardiomyocyte cultures for the quantitative detection of compound induced effects. This could pave the way for more predictive *in vitro* chronic/repeated dose cardiotoxicity testing assays.

1. Introduction

Based on the tremendous progress in stem cell research, human stem cell derived cardiomyocytes offer a great opportunity for clinical applications *e.g.* cell based therapies (Burridge et al., 2012) but also support *in vitro* research like pathology models (Robertson et al., 2013), and novel drug development, especially drug safety testing (Kattman et al., 2011; Lian et al., 2010). This could prevent withdrawal of approved therapeutics due to unexpected negative side effects on the human heart (Braam et al., 2010; Khan et al., 2013; Redfern et al., 2003; Robertson et al., 2013). For traditional preclinical *in vitro* drug studies, genetic-modified non-cardiac or non-human cardiac cells are used in short-term acute toxicity tests or involve the use of animals. All these models have critical drawbacks like its high artificial character and/or the critical extrapolation of animal cells derived data to humans (Lu et al., 2001; Olson et al., 2000; Yang et al., 2014). Thus, especially human induced pluripotent stem cell (hiPSC) derived cardiomyocytes provide a promising cell source.

Depending on the application, there are several demands on stem cell derived cardiomyocytes. First, differentiation to cardiomyocyte cultures should lead to a high enrichment of cardiomyocytes without unwanted cell types like fibroblasts and cell types of endodermal or ectodermal origin. The state of the art for differentiation is the time-dependent modulation of the Wnt signalling pathway by growth factors or small molecules on 2D cultures (Burridge et al., 2014; Paige et al., 2010) but up to now the yield of cardiomyocytes still varied depending

* Correspondence to: Centre for Biotechnology and Biomedicine, Universität Leipzig, Division of Molecular Biological-Biochemical Processing Technology, Deutscher Platz 5, 04103 Leipzig, Germany.
E-mail address: andrea.robitzki@bbz.uni-leipzig.de (A.A. Robitzki).

https://doi.org/10.1016/j.bios.2018.10.061
Received 30 June 2018; Received in revised form 18 October 2018; Accepted 27 October 2018
Available online 29 October 2018

on hPSC-line and protocol (Burridge et al., 2012; Laflamme et al., 2007; Lian et al., 2013).

Second, maturation is the biggest actual challenge for hPSC derived cardiomyocytes. Despite using state of the art differentiation protocols, the majority of functional cardiomyocytes represents a more foetal like phenotype with distinct differences to adult cardiomyocytes for important structural characteristics (Yang et al., 2014) and moreover, ion channels and signal pathways like for the calcium homeostasis (Keung et al., 2014; Yang et al., 2014).

Third, long-term stability of hiPSC derived cardiomyocyte cultures is a critical point, especially for *in vitro* studies of drug-induced chronic and repeated dose cardiotoxicity (Khan et al., 2013). While most cardiac cultures are already widely used for short-term *in vitro* experiments within hours or single days (Braam et al., 2010; Maddah et al., 2015; Redfern et al., 2003) there is a lack of long-term hiPSC derived cardiomyocyte models that provide the high demands for feasibility, stability and reproducibility of electrophysiological activity as well as sensitive response to drugs over weeks or month. In this context, there is also a great demand for label-free non-invasive monitoring techniques that provide robust and quantitative parameter for analysis of the differentiation and maturation process and ideally of cellular alterations in cardiotoxicity and drug testing assays. While simple planar microelectrodes are available for a long time and widely used for the bioelectronic analysis of monolayer cardiomyocyte cultures on top of the electrodes (Aravanis et al., 2001; Krinke et al., 2009; Takasuna et al., 2017), the sensitive and robust bioelectronic monitoring of 3D cultures is still demanding. Therefore, special 3D measurement chambers (Kloss et al., 2008; Zhang et al., 2018) were developed. Furthermore, modified and vertical electrode arrays were developed to improve the situation (Frank et al., 2018; Shi et al., 2018, 2017). In this context, we want to use electrophysiological recording and impedance spectroscopy in combination with microelectrode arrays (2D) and microcavity arrays (3D) for quantitative long-term monitoring of 2D and 3D cardiomyocyte cultures.

2. Methods and materials

2.1. hiPSC culturing and human cardiomyocyte differentiation

Human induced pluripotent stem cells IMR90C01 (Fig. S1) were cultured as previously described (Ludwig et al., 2006) (detailed information in Supplemental material). Differentiation was performed as previously described (Lian et al., 2013). Briefly, differentiation was initiated at 80–95% confluency by adding basal medium (RPMI 1640, 2% B-27 without insulin,1% GlutaMAX™, (all from Life Technologies, Germany)) with 1 μM CHIR98014 (Santa Cruz Biotechnology, Germany) for 24 h. Afterwards, medium was changed every second day without CHIR98014. On day 3, 1 μM IWP-4 was added (Miltenyi Biotec, Germany). Two days later, medium was changed without adding IWP-4 for two days. For long-term culturing, cells were maintained in low-serum medium (DMEM/F-12 1:1, 2 mM GlutaMAX™, 1% NEAA, 0.2% Pen/Strep (all from Life Technologies, Germany), 2% FCS (Lonza, BioWhittaker, Germany), 50 μg/mL ascorbic acid (Carl Roth, Germany), 0.1 mM β-mercaptoethanol (Sigma-Aldrich, Germany) with medium exchange every second day.

2.2. Cell reaggregation

2D cultures were dissociated with 0.25% trypsin-EDTA (Life Technologies, Germany) and 0.5 mg/mL DNase I (AppliChem, Germany) for 30 min at 37 °C followed by mechanical separation. After centrifugation at 500 × *g* for 5 min, single cells were resuspended in

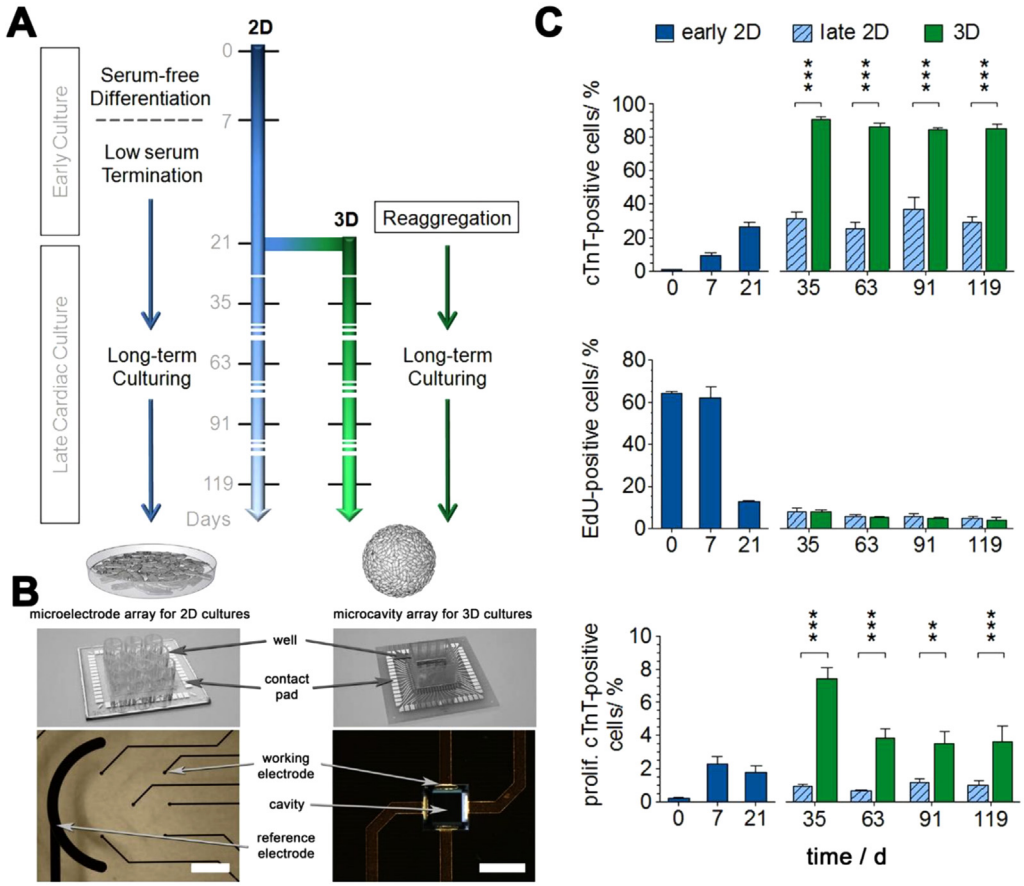

Fig. 1. Combined protocol for generation of advanced 3D cardiomyocyte cultures. (A) Scheme for cell differentiation and comparison of 2D and 3D cardiomyocyte cultures starting from hiPSC IMR90C01 monolayer culture. (B) Different array types for bioelectronic monitoring of 2D (microelectrode array) and 3D (microcavity array) cardiomyocyte cultures (scale bar microelectrode array: 1 mm; microcavity array: 400 μm). (C) Flow cytometric analysis of cardiac troponin T (cTnT) to evaluate the content of cardiac cells. Using proliferation marker EdU proliferation rate (EdU-positive cells) and proliferating cardiomyocytes (cTnT/EdU-double positive cells) could be determined. (n = 3 independent experiments).

low-serum medium with 10 µM ROCK-inhibitor Y-27632 (Santa Cruz Biotechnology, Germany) and seeded in 96-well plates with V-bottom (Thermo Fisher Scientific, Nunc, Germany) with 50,000 cells in 200 µl per well. Afterwards, plates were centrifuged at 1000 × *g* and 4 °C for 10 min. Next day, medium was changed to remove ROCK-inhibitor. After three more days, generated clusters were transferred to U-bottomed 96-well plates (Greiner Bio One, Germany) for long-term culturing. Every three to four days, low-serum medium was exchanged.

2.3. Electrochemical impedance spectroscopy

Impedance spectra were recorded as previously described (Jahnke et al., 2013). Therefore, 2D culture (day 21) were dissociated as described for reaggregation and seeded on planar microelectrode arrays. Impedance spectra were recorded using a self-developed 60 channel multiplexer in combination with a high precision impedance analyser (ISX-3, Sciospec Scientific Instruments, Germany). For analysis, the relative impedance (|Z|sample − |Z|blank)/|Z|blank × 100% was calculated and the relative impedance maximum were extracted and traced over time. To minimize variations from each cluster six impedance spectra were recorded (each electrode against each other) and spectra maxima were averaged.

2.4. Field potential recording

Field potentials were recorded using the MEA/MCA as described for impedance spectroscopy. MEA/MCA was placed in a heated (37 °C) MEA1060BC amplifier system (Multichannel Systems, Germany). Recording was performed at a sampling rate of 4 kHz for 15 min (long-term measurements) or one hour (drug testing). For action potential detection (contraction rate analysis) and action potential duration (APD) determination a self-developed Matlab software was used (Jahnke et al., 2013). The QT interval related APD was corrected according to Bazett's formula. Cluster treatment with (-)-isoproterenol hydrochloride (Sigma-Aldrich, Germany) and E4031 (Santa Cruz Biotechnology, Germany) was performed as an accumulative experiment by adding next higher concentration every hour.

2.5. Statistics

Statistic data analysis was done using GraphPad Prism version 5 (GraphPad Software, USA). Data represented as mean ± SEM, unless otherwise indicated. Nonlinear regression fit for agonists/antagonists (three parameters) were used for EC_{50} value determination. One group analysis were performed by 1D ANOVA and Dunnett post hoc test, multiple group comparisons were done by 2D ANOVA and Bonferroni post hoc test, and between two means *t*-test (two-tailed) was used. Statistically differences between two means with $p < 0.05$ were regarded as statistically significant (*), $p < 0.01$ very significant (**), and $p < 0.001$ extremely significant (***).

3. Results and discussion

3.1. Combined 2D differentiation and forced reaggregation leads to highly enriched long-term stable human cardiomyocyte clusters

To obtain an advanced reproducible 3D cardiomyocyte culture model we combined Wnt signalling pathway modulator based differentiation of 2D hiPSC cultures (IMR90C01 cell line) with a 3D culturing system (Fig. 1A). The initially differentiated 2D cultures were dissociated on day 21 and single cells were reaggregated to generate uniform spheric clusters. For comparison of cardiac differentiation and cardiac maturation, 2D and 3D cardiomyocyte cultures were long-term cultured for further 98 days (Fig. 1A). For the long-term bioelectronic

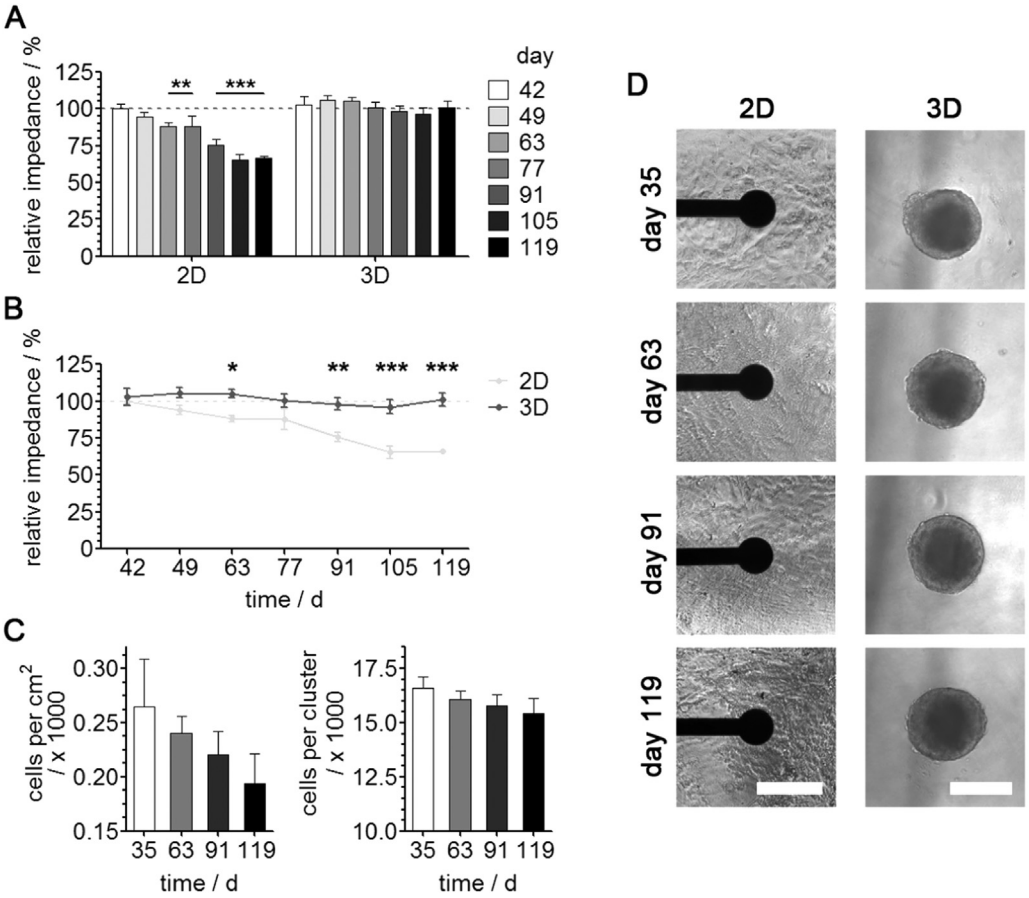

Fig. 2. Impedance spectroscopy prove cellular resistance changes of 2D and. 3D over time. (A) At indicated time points comparative analysis of relative impedance of on microelectrode array reseeded 2D as well as 3D culture using microcavity array (normalised to day 35, dashed line) as well (B) between each other were performed (n = 3 independent experiments, a(2D) = 3 9w7en microelectrode array/ a(3D) = 30 cluster). (C) Cell amount of 2D and 3D culture were analysed by counting single cells. For 2D amount was show as cells per cm^2 and for 3D culture as cells per singularised cluster. Data shown from independent experiments with n(2D) = 3 (a = 3 wells) and n(3D = 10 (a ≥ 30 cluster). (D) Representative pictures are shown from 2D and 3D cultures (2D scale bar 200 µm; 3D scale bar 400 µm).

monitoring of both 2D and 3D cultures, specific optimized array types were used (Fig. 1B). In detail, microelectrode arrays with six electrodes (100 µm diameter) per well were used for 2D cardiomyocyte cultures and microcavity arrays (Fig. S2) for 3D cardiomyocyte cultures.

First, flow cytometric analysis was performed to determine cardiac marker troponin T (cTnT) positive cells as well as the proliferation rate (Fig. 1C). During the first weeks of differentiation, the amount of $cTnT^+$ cells constantly increased up to 31%. First spontaneous beating areas were reproducibly detected between day 9 and 15 (Movie S1). Quantitative analysis of late cardiomyocyte 2D cultures showed no significant changes of $cTnT^+$ cells beyond day 21. Therefore, we dissociated 2D cultures and reaggregated them to cardiomyocyte clusters at day 21. The mechanical reaggregation led to highly enriched cardiomyocyte clusters with up to 91% $cTnT^+$ cells at day 35 with no significant changes over the analysed time range of 84 days. Although the reason for this cardiomyocyte enrichment is still unclear, there is a prior study that describes a comparable effect (Nguyen et al., 2014). In this study the authors claim that a higher density of the cardiomyocytes leads to the enrichment during the forced aggregation step. It is known that during cardiomyocyte differentiation the proliferation rate decreases from progenitor cells to early and further more to matured cardiomyocytes (Robertson et al., 2013; Zhang et al., 2009). Therefore, we investigated the amount of proliferating cells in 2D and 3D cultures. During initiation of differentiation, until day 7, a high amount of proliferating cells (> 60%) was detectable. At later time points, the amount of proliferating cells decreased drastically in average down to 12.4% (day 21) and at least to < 5% (day 119) with no significant differences between 2D and 3D cultures. More interestingly, the amount of proliferating $cTnT^+$ cells was up to fivefold higher in 3D culture. Clusters exhibited not only a highly enriched cardiomyocyte culture; they revealed already 4 days after reaggregation a highly reproducible spheroid shape (Fig. S3A,B) with a diameter of 445.7 ± 5.1 µm at day 35 that kept stable up to day 119 of culturing (Fig. S3C). Using impedance spectroscopy and cell number analysis we investigated for changes like proliferation and cell death as well as changes in culture/tissue density that can be detected by an increase or even decrease of

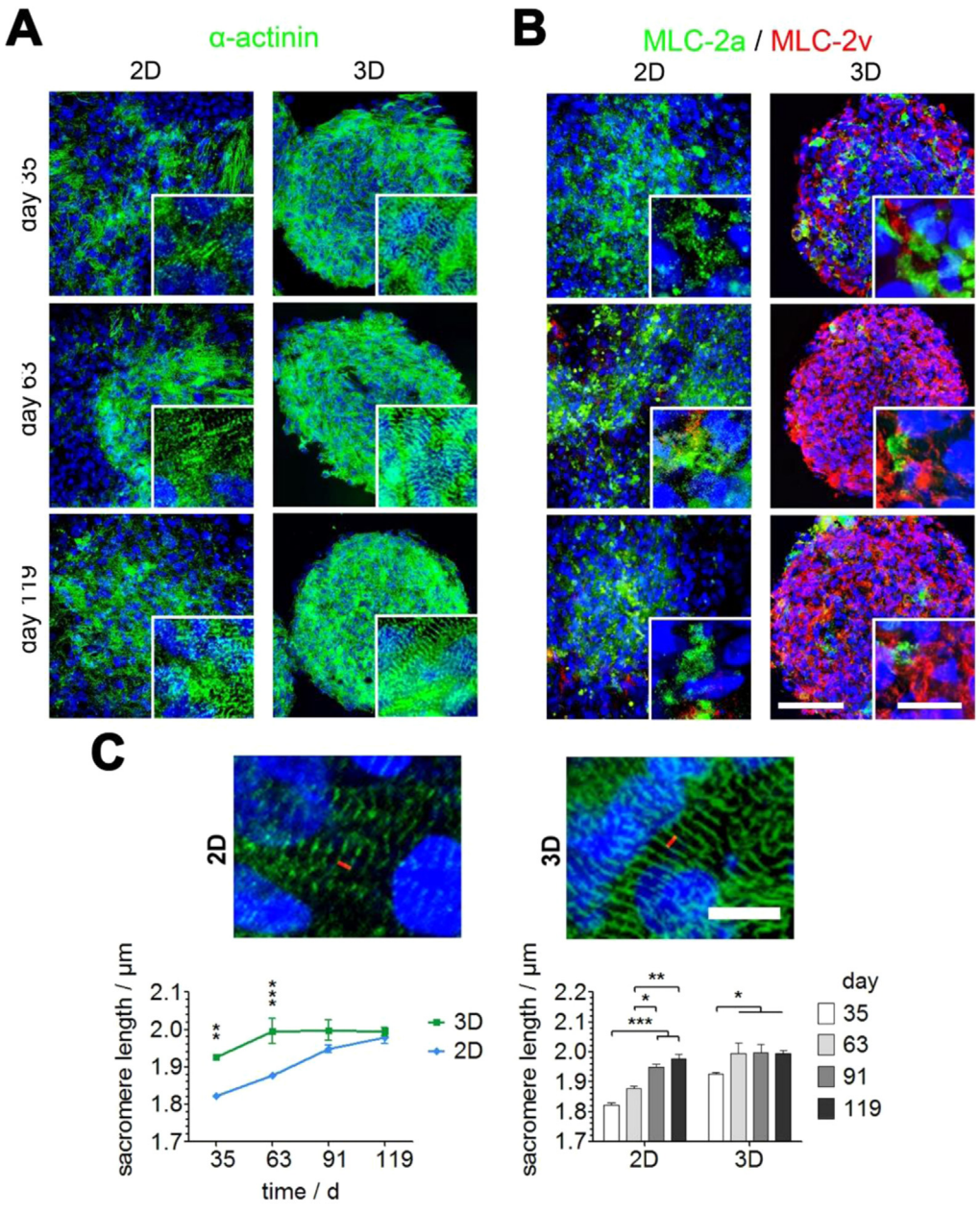

Fig. 3. 3D cultures showing advanced expressions of cardiac-specific markers. 2D and 3D cultures were harvested at same indicated time points (day 35, 63, and 119). Representative immunocytochemical analysis of (A) filament protein α-actinin (green) and (B) MLC-2a (green)/MLC-2v (red). Nuclei were stained by DAPI (blue). (scale bar 200 µm; magnification 20 µm). (C) Sarcomere length analysis of 2D and 3D culture model. Using sarcomeric α-actinin staining, sarcomere lengths were determined (red line) as shown for day 119. Statistical analysis of changes in distance between Z-lines in both culture models were analysed to each other as well over time from three independent experiments with each 30 replicates. (scale bar 10 µm). (For interpretation of the references to color in this figure legend, the reader is referred to the web version of this article).

relative impedance, respectively (Jahnke et al., 2013).

Supplementary material related to this article can be found online at doi:10.1016/j.bios.2018.10.061.

In correlation with the cluster cell number analysis (Fig. 2C) the relative impedance showed no significant changes over the whole measurement period (Fig. 2A). Moreover, clusters were characterised by synchronous contractions over the whole cluster until day 119 (Movie S2). In contrast, normalised relative impedance of 2D cultures declined significantly after 63 days (Fig. 2A). This decrease was also significantly different to 3D (Fig. 2B). Cell amount analysis and microscopic documentations (Movie S3) confirmed that 2D cell layers became instable as cell number decreased over time (Fig. 2C,D). Taken together, our new protocol allowed an efficient and reproducible generation of highly enriched and long-term stable human cardiomyocyte 3D cultures, which could be tracked and quantified using microcavity array based impedimetric monitoring.

Supplementary material related to this article can be found online at doi:10.1016/j.bios.2018.10.061.

3.2. 3D culturing leads to an accelerated maturation and cardiac subtype switch

To investigate cardiac maturation, the expression and localization of cardiac specific proteins was analysed by immunocytochemical staining for α-actinin (Fig. 3) and cardiac troponin T (Fig. S5). At day 7 first observations of myofilament protein troponin T revealed expression in 2D cultures in small areas (Fig. S5). Over time α-actinin as well as troponin T expression increased but many cells of the 2D culture still lacked the expression of these cardiac structure proteins (Fig. 3). Comparing 2D and 3D cardiac cultures, the amount of positive cells correlated with the flow cytometric analysis of troponin T (see Fig. 1). Notable there was an abundant expression of both proteins in the whole cluster in comparison to 2D cultures (Fig. 3 and S4). Thus, the high expression and homogeneous distribution of myofilament proteins highlighted the enrichment of cardiomyocytes in the clusters. Analysis of vimentin, an intermediate filament that occurs in non-cardiac cells of mesenchymal origin (Jahnke et al., 2013; Thavandiran et al., 2013; Zhang et al., 2012a) revealed areas in 2D cultures with high expression (Fig. S6). In contrast, 3D culture exhibited only a residual non-cardiac cells most likely smooth muscle cells but almost no fibroblasts (Fig. S6). The maturation process of cardiac tissue is not only marked by structural protein expression but also by the abundant distinct expression of gap junctions (Lundy et al., 2013; Mihic et al., 2014; Rao et al., 2013; Zhang et al., 2012b). Immunochemical staining of connexin43, the most dominant gap junction in human heart, and cytochrome C oxidase, a mitochondria marker, proved that at all times 3D culture exhibited a higher and well distributed expression of both marker proteins (Fig. S4). Next, we analysed immunocytochemical co-staining of the

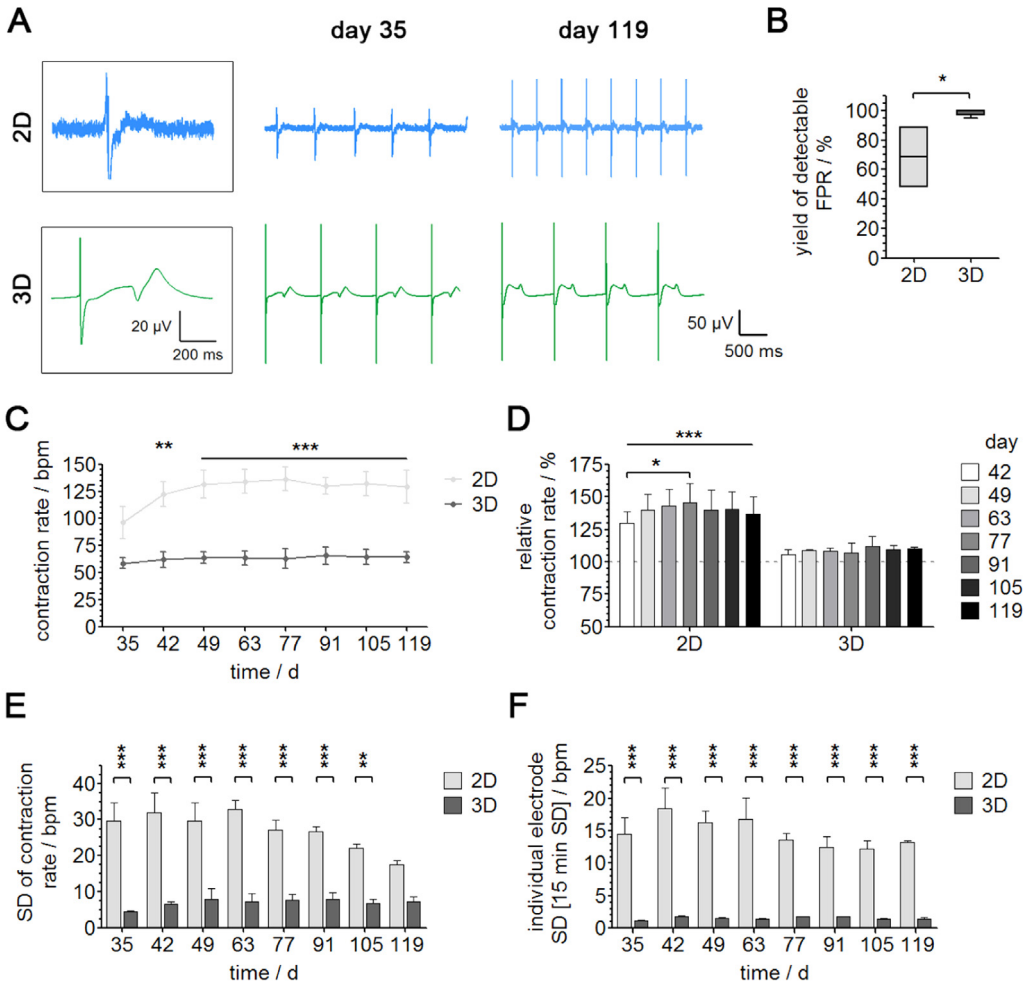

Fig. 4. Electrophysiological characterisation of 2D *vs.* 3D long-term culturing. (A) Signal quality from representative 2D and 3D field potential derived action potential recordings at early (day 35) and late time points (day 119). (B) Yield of detectable field potential recordings on day 35 (n = 4 independent differentiations). Long-term contraction rate analysis (C) between 2D and 3D as well as (D) over time (normalised to day 35, dashed line). (E) Standard deviation of contraction rate and (F) individual electrode standard deviation of contraction rate derived from 15 min recordings (within a experimental group). (n = 3 independent experiments).

myosin light chain 2 atrial (MLC-2a, green) and ventricular isoform (MLC-2v, red) (Fig. 3). It is known, that the expression pattern of MLC-2a and -2v in cardiomyocytes refer to atrial or ventricular subtypes in matured cardiomyocytes. At early maturation stages both subtypes are MLC-2a positive and MLC-2v negative with a switch from MLC-2a to MLC-2v for the ventricular subtype during cardiac development and maturation (Tiburcy et al., 2011; Zhang et al., 2012b). At early time points (until day 35) in 2D cultures, only small amounts of MLC-2a were detectable and no MLC-2v could be observed (Fig. 3). However, late 2D cultures showed more distinct MLC-2a positive structures and very low expression of locally isolated MLC-2v. For 3D cultures, a switch in protein expression from similar MLC-2a/-2v ratios at the beginning toward a more pronounced MLC-2v expression was found during culturing. Thus, cardiac subtype marker analysis revealed an atrial subtype cardiomyocyte character for 2D cultures while in 3D cultures nearly all cardiomyocytes switched towards exclusive and abundant expression of ventricular subtype after 63 days. The amount and organization of striated pattern of sarcomers as well as their length extension are markers of cardiac maturation (Lundy et al., 2013; Zhang et al., 2013). Therefore, we analysed structure proteins α-actinin and cardiac troponin T by immunostaining. In contrast to 2D cultures, 3D cultures showed more characteristic, discrete and well-organised sarcomeric structures. Hence, the sarcomere length was analysed based on the α-actinin staining (Fig. 3C). Already 14 days after reaggregation, in clusters significant longer sarcomeres than in 2D cultures were measured. Interestingly, in 2D cultures the sarcomere length increased up to day 119 of culturing, reaching comparable length to 3D cultures. However, 3D cluster maturation was much faster reaching sarcomere length up to 2.0 µm already at day 63 of culture revealing an accelerated maturation of cardiomyocytes in 3D cultures with a time advance of at least 2 month.

3.3. Gene expression analysis reveals a more adult like cardiomyocyte phenotype for human 3D cardiac cultures

For a more detailed analysis of cardiac maturation relevant markers, 2D and 3D culture gene expression was analysed by qRT-PCR (Fig. S7 and Table S1). This included the cardiac structure proteins cardiac troponin T type 2 (*TNNT2*), myosin light chain 2 ventricular (*MLC-2v*), and myomesin 2 (*MYOM2*) (Kamakura et al., 2013; Yang et al., 2014). Furthermore, genes encoding for proteins *e.g.* involved in ion transport and homeostasis (Blazeski et al., 2012; Bosman et al., 2013; Rao et al., 2013; Robertson et al., 2013; Yang et al., 2014), the ryanodine receptor 2 (*RYR2*), Ca(2 +)-ATPase (*ATP2A2*), phospholamban (*PLN*), calsequestrin 2 (*CASQ2*), and caveolin 3 (*CAV3*) were analysed. For grading the relative mRNA expression levels, reference samples obtained from foetal and adult human heart samples were additionally analysed (Fig. 5). The relative expression of all specific cardiac markers increased up to day 21. From day 21 on, gene expression for *MLC-2v*, *CASQ2*, *CAV3,* and *MYOM2* was further upregulated in monolayer cultures but could not reach same levels compared to 3D culture. In late 2D culture, gene expression level of *TNNT2* as well as *RYR2*, *ATP2A2*, and *PLN* maintained stable. For the same markers in 3D cultures, gene expression raised over time especially for *MYOM2*, *ATP2A2*, *CASQ2*, and *CAV3*. In comparison to the human heart reference samples, in 2D cultures the structure protein related gene expression levels of *TNNT2* and *MLC-2v* were extremely low and never reached levels of neither foetal nor adult heart (both > tenfold higher). Although, in 3D cultures the expression levels of *TNNT2* and *MLC-2v* did not reached the gene expression level of foetal and adult samples (both > twofold higher), they were significantly higher than 2D (up to eightfold). More strikingly, for *MYOM2* as well as *RYR2, ATP2A2, PLN,* and *CAV3* gene expression in 3D cultures reached expression levels of the human heart reference samples, while in 2D cultures gene expression was much lower. Additional, qRT-PCR revealed a correlative expression tendency from foetal to adult human heart samples under the thesis that 3D cultures are more matured than 2D cultures for all tested genes as well as comparable expression levels of the 3D cultures to the human heart reference samples. Thus, gene expression analysis confirms results from immunocytochemical stainings that 3D cultures represent a more matured cardiomyocyte phenotype.

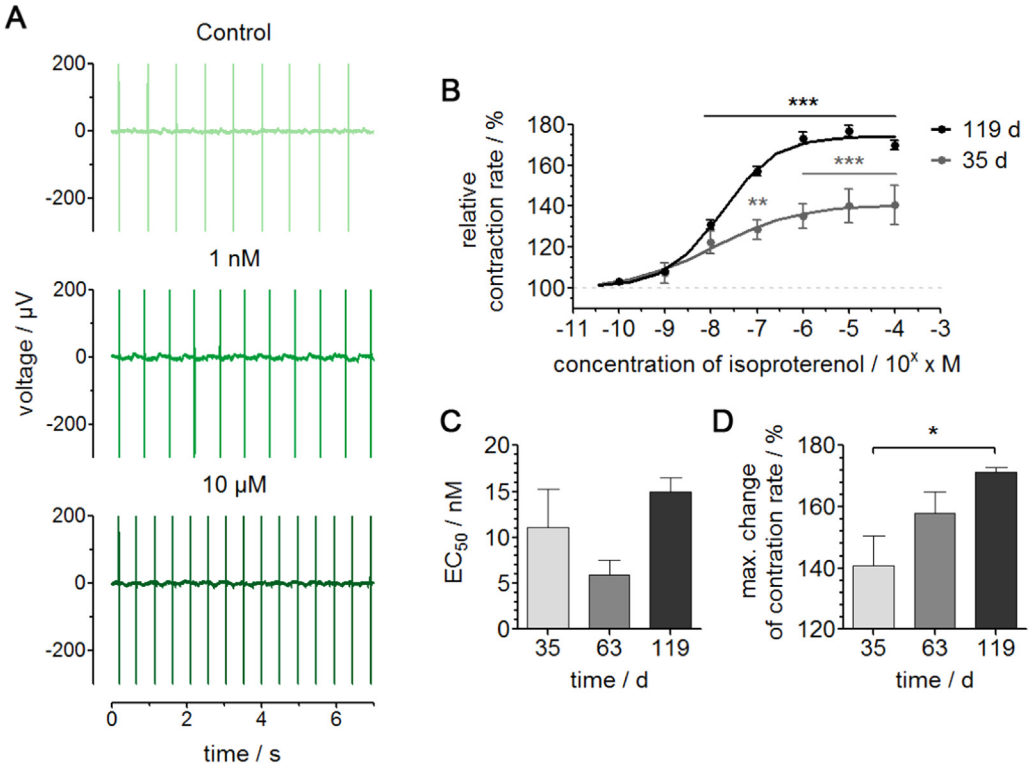

Fig. 5. Long-term characterisation of chronotropic effect of β-adrenergic agonist isoproterenol on tissue-like cardiomyocyte clusters at early (day 35), late (day 63), and very late (day 119) time point. (A) Demonstrating active substance influence on contraction rate representative field potential recordings after application of increasing isoproterenol concentrations at day 63. (B) Active drug concentration response curves from one representative experiment (day 35 and 119). Statistical analysis of the (C) EC_{50} values and (D) maximal changes of contraction rate. (n = 3 independent experiments).

3.4. Human 3D cardiomyocyte cultures show advanced electrophysiological characteristics

Essential for long-term *in vitro* experiments in the field of chronic safety assessment, pathological model studies, and drug development is a high yield of functional, stable and reproducible electrophysiological active cultures. To analyse the electrophysiology we used microelectrode arrays for 2D and microcavity array for 3D cardiomyocyte cultures (See Fig. 1B) for recording the extracellular field potential of the attached cells and clusters (Jahnke et al., 2013). With regard to signal strength and quality at early time points, for 2D cultures only very small amplitudes could be detected (Fig. 4A). While amplitudes increased over time, it was often not possible to accurately detect the action potential duration (repolarisation signal), which is important for the action potential duration (APD) analysis. In contrast, high quality signals from 3D cultures allowed feasible determination of the APD (Fig. 4A). Furthermore, the yield of individual wells (2D culture) with electrophysiological activity was only 67% (Fig. 4B). In contrast, 99% of all cardiomyocyte clusters showed synchronized contractility over the whole cluster (Movie S4) and revealed electrophysiological activity. Next, we analysed the long-term electrophysiological stability. 3D cultures showed a stable contraction rate between 58.5 and 65.8 beats per minute (bpm) over 84 days of monitoring (Fig. 4C). In contrast, starting with 96.3 bpm at day 35, contraction rate of 2D cultures was significantly increased afterwards (up to 136.4 bpm; Fig. 4A). Normalising data to day 35, statistical analysis exhibit no significant change in the contraction rate for 3D over time (Fig. 4D). In contrast, for 2D cultures contraction rate increased significantly. To analyse the variability of contraction rate within each differentiation standard deviation of the contraction rate from each independent experiment (derived from replicate statistics) was analysed (Fig. 4E). 2D cultures revealed a significant higher standard deviation than 3D cultures up to 105 days of culture. Interestingly, variability of the contraction rate for 2D cultures declined during culturing but was still twofold higher than for 3D cultures up to day 119. Moreover, we analysed the variance of contraction rate for each individual unit (well/cluster) within 15 min of recording for each experiment (Fig. 4F). The individual contraction rate variances of 2D cultures were significant seven- to twelvefold higher in comparison to 3D cultures. Altogether, culturing hiPS cell derived cardiomyocytes in a 3D model led to a stable contracting cell population whereas the 2D cultivation led to increased and more fluctuating contraction rates over time. This unique property from new developed 3D culturing system provides a new cardiomyocytes model for long-term pharmaceutical screenings.

Supplementary material related to this article can be found online at doi:10.1016/j.bios.2018.10.061.

3.5. 3D cardiac cultures show high sensitivity towards contraction rate and action potential duration affecting reference compounds

To demonstrate the sensitivity of our 3D cultures with regard to beta-adrenergic signalling pathway (chronotropic effects), the well-known beta-adrenergic agonist isoproterenol was accumulatively applied (Fig. 5). As negative control acetaminophen (from 10^{-9} to 10^{-2} M), a pain reliever with no known influence on contraction, was used (Fig. S8). Treatment with acetaminophen resulted in no significant contraction rate alterations. Application of β-adrenergic agonist significantly induced a contraction rate increase at 100 nM at day 35 and already at 10 nM at day 119 (Fig. 5B). Nevertheless, determined EC_{50} for each time point did not changed significantly (day 35: 11.13 ± 4.2 nM, day 63: 5.87 ± 1.7 nM, day 119: 14.99 ± 1.5 nM) (Fig. 6C). Interestingly, a higher contraction rate change at later time points was observed (Fig. 5D) which could be caused by a more matured β-adrenergic signal pathway. Maximal change of contraction rate significantly increased from day 35 to day 119 (140.6 ± 9.9% to 171.4 ± 1.5%). As done for isoproterenol, we analysed the reference compound E4031 that blocks the *HERG* channel thereby inducing an increase of the action potential duration (APD), which is correlated to QT-prolongation and therefore, arrhythmias (Fig. 6) (Khan et al., 2013; Ponte et al., 2010; Yamazaki et al., 2012). First, we proved that the responsible target, the voltage-gated potassium channel (*HERG),* is present by qRT-PCR (Fig. 6A). The statistical analysis revealed that between day 35 and 63 or 119 gene expression increased about 30% (53%). In comparison to human heart reference samples, 3D cultures were more similar to foetal sample at day 35 but later to adult heart samples. Analysing the recorded field potential after E4031 application, the effect on the action potential duration could be detected (Fig. 6B). Increasing the E4031 concentration led to a significant prolonged action potential duration at day 35 (10 nM) up to day 119 (1 nM) (Fig. 6C). Statistical analysis of three independent experiments proved that the EC_{50} changed over time. On day 35 we could determine an EC_{50} of 19.58 ± 5.3 nM. Already four weeks later the EC_{50} value significantly decreased down to 1.56 ± 0.3 nM and kept stable up to culturing day 119 (1.59 ± 0.3 nM; Fig. 6D). Although the sensitivity to

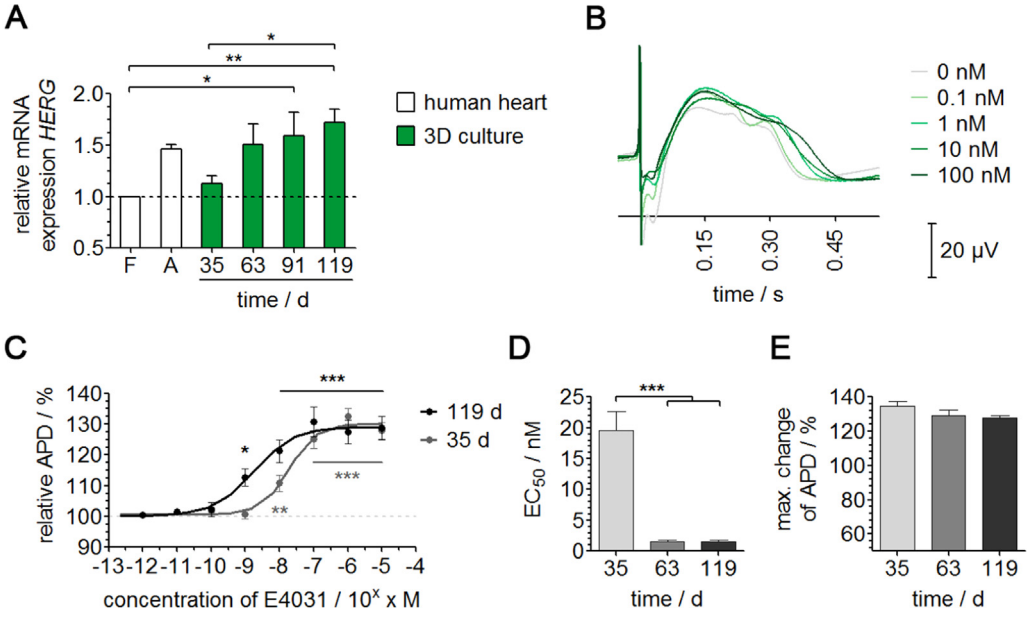

Fig. 6. Long-term characterisation of E4031 effect on the action potential duration (APD). (A) qPCR analysis of potassium voltage-gated channel gene (*HERG)* expression over time. Human foetal heart [F] and adult heart [A] samples were used as gene expression references. Quantification was done by normalising to housekeeping gene *hGAPDH* and human foetal heart sample. (n = 3 independent experiments). (B) Representative field potential derived action potential recordings after application of increasing concentrations of E4031 at day 35. (C) Representative concentration response curves of one experiment (n = 6 clusters, day 35 and 119). Statistical analysis of determined (D) EC_{50} values and (E) maximal changes of APD interval. (n = 3 independent experiments).

E4031 increased, the maximal change of the action potential duration remained stable over time (Fig. 6E).

4. Conclusion

Taken together, we demonstrated that the Wnt signalling pathway modulation based differentiation of hiPSC cultures to cardiomyocytes reveals certain differences between 2D and 3D cardiomyocyte clusters. There are several biological effects like a highly enrichment of cardiomyocytes in 3D cultures and furthermore, a phenotype switch from atrial to ventricular cardiomyocytes without further purification or selection. Moreover, 3D cultures showed an accelerated maturation with a time gain of more than 60 days when compared to 2D cultures. Furthermore, using planar microelectrode arrays for 2D cultures and microcavity arrays for 3D cultures allowed the long-term bioelectronic monitoring and comparison. Using these techniques a reproducible superior long-term stability of the 3D cultures for 100 days could be quantitatively proved. Moreover, impedimetric and electrophysiological monitoring could be used to analyse sensitive reactions to chronotropic and QT-prolonging reference compounds. This is an important step forward for using such bioelectronic monitoring systems for hiPSC derived cardiomyocytes. More strikingly, these techniques and shown applications could pave the way to establish them as reference methods for quality control of stem cells and thereof derived specific cell types as well as for *in vitro* applications like pathology model development for research and drug development as well as safety assessment or *in vivo* applications like cell-based therapies.

Acknowledgments

This work was funded by European Commission Seventh Framework Programme (FP7/2007-2013 and Cosmetics Europe based on the Grant Agreement No. 266753 (Scr&Tox)). The image acquisition facility (confocal microscope) and the impedance analyser were funded by the Free State of Saxony and the European Union (SMWK/EFRE). We thank Ronny Frank for drawing cell schemes.

Appendix A. Supporting information

Supplementary data associated with this article can be found in the online version at doi:10.1016/j.bios.2018.10.061.

References

Aravanis, A.M., DeBusschere, B.D., Chruscinski, A.J., Gilchrist, K.H., Kobilka, B.K., Kovacs, G.T., 2001. Biosens. Bioelectron. 16 (7–8), 571–577.
Blazeski, A., Zhu, R., Hunter, D.W., Weinberg, S.H., Boheler, K.R., Zambidis, E.T., Tung, L., 2012. Prog. Biophys. Mol. Biol. 110 (2–3), 178–195.
Bosman, A., Sartiani, L., Spinelli, V., Del Lungo, M., Stillitano, F., Nosi, D., Mugelli, A., Cerbai, E., Jaconi, M., 2013. Stem Cells Dev. 22 (11), 1717–1727.
Braam, S.R., Tertoolen, L., van de Stolpe, A., Meyer, T., Passier, R., Mummery, C.L., 2010. Stem Cell Res. 4 (2), 107–116.
Burridge, P.W., Keller, G., Gold, J.D., Wu, J.C., 2012. Cell Stem Cell 10 (1), 16–28.
Burridge, P.W., Matsa, E., Shukla, P., Lin, Z.C., Churko, J.M., Ebert, A.D., Lan, F., Diecke, S., Huber, B., Mordwinkin, N.M., Plews, J.R., Abilez, O.J., Cui, B., Gold, J.D., Wu, J.C., 2014. Nat. Methods 11 (8), 855–860.
Frank, R., Klenner, M., Zitzmann, F.D., Schmidt, S., Ruf, T., Jahnke, H.-G., Denecke, R., Robitzki, A.A., 2018. Electrochim. Acta 259, 449–457.
Jahnke, H.G., Steel, D., Fleischer, S., Seidel, D., Kurz, R., Vinz, S., Dahlenborg, K., Sartipy, P., Robitzki, A.A., 2013. PLoS One 8 (7), e68971.
Kamakura, T., Makiyama, T., Sasaki, K., Yoshida, Y., Wuriyanghai, Y., Chen, J., Hattori, T., Ohno, S., Kita, T., Horie, M., Yamanaka, S., Kimura, T., 2013. Circ. J.: Off. J. Jpn. Circ. Soc. 77 (5), 1307–1314.
Kattman, S.J., Koonce, C.H., Swanson, B.J., Anson, B.D., 2011. J. Cardiovasc. Transl. Res. 4 (1), 66–72.
Keung, W., Boheler, K.R., Li, R.A., 2014. Stem Cell Res. Ther. 5.
Khan, J.M., Lyon, A.R., Harding, S.E., 2013. Br. J. Pharmacol. 169 (2), 304–317.
Kloss, D., Kurz, R., Jahnke, H.G., Fischer, M., Rothermel, A., Anderegg, U., Simon, J.C., Robitzki, A.A., 2008. Biosens. Bioelectron. 23 (10), 1473–1480.
Krinke, D., Jahnke, H.G., Pänke, O., Robitzki, A.A., 2009. Biosens. Bioelectron. 24 (9), 2798–2803.
Laflamme, M.A., Chen, K.Y., Naumova, A.V., Muskheli, V., Fugate, J.A., Dupras, S.K., Reinecke, H., Xu, C., Hassanipour, M., Police, S., O'Sullivan, C., Collins, L., Chen, Y., Minami, E., Gill, E.A., Ueno, S., Yuan, C., Gold, J., Murry, C.E., 2007. Nat. Biotechnol. 25 (9), 1015–1024.
Lian, Q., Chow, Y., Esteban, M.A., Pei, D., Tse, H.F., 2010. Thromb. Haemost. 104 (1), 39–44.
Lian, X., Zhang, J., Azarin, S.M., Zhu, K., Hazeltine, L.B., Bao, X., Hsiao, C., Kamp, T.J., Palecek, S.P., 2013. Nat. Protoc. 8 (1), 162–175.
Lu, H.R., Marien, R., Saels, A., De Clerck, F., 2001. J. Cardiovasc. Electrophysiol. 12 (1), 93–102.
Ludwig, T.E., Bergendahl, V., Levenstein, M.E., Yu, J., Probasco, M.D., Thomson, J.A., 2006. Nat. Methods 3 (8), 637–646.
Lundy, S.D., Zhu, W.Z., Regnier, M., Laflamme, M.A., 2013. Stem Cells Dev. 22 (14), 1991–2002.
Maddah, M., Heidmann, J.D., Mandegar, M.A., Walker, C.D., Bolouki, S., Conklin, B.R., Loewke, K.E., 2015. Stem Cell Rep. 4 (4), 621–631.
Mihic, A., Li, J., Miyagi, Y., Gagliardi, M., Li, S.H., Zu, J., Weisel, R.D., Keller, G., Li, R.K., 2014. Biomaterials 35 (9), 2798–2808.
Nguyen, D.C., Hookway, T.A., Wu, Q., Jha, R., Preininger, M.K., Chen, X., Easley, C.A., Spearman, P., Deshpande, S.R., Maher, K., Wagner, M.B., McDevitt, T.C., Xu, C., 2014. Stem Cell Rep. 3 (2), 260–268.
Olson, H., Betton, G., Robinson, D., Thomas, K., Monro, A., Kolaja, G., Lilly, P., Sanders, J., Sipes, G., Bracken, W., Dorato, M., Van Deun, K., Smith, P., Berger, B., Heller, A., 2000. Regul. Toxicol. Pharmacol.: RTP 32 (1), 56–67.
Paige, S.L., Osugi, T., Afanasiev, O.K., Pabon, L., Reinecke, H., Murry, C.E., 2010. PLoS One 5 (6), e11134.
Ponte, M.L., Keller, G.A., Di Girolamo, G., 2010. Curr. Drug Saf. 5 (1), 44–53.
Rao, C., Prodromakis, T., Kolker, L., Chaudhry, U.A.R., Trantidou, T., Sridhar, A., Weekes, C., Camelliti, P., Harding, S.E., Darzi, A., Yacoub, M.H., Athanasiou, T., Terracciano, C.M., 2013. Biomaterials 34 (10), 2399–2411.
Redfern, W.S., Carlsson, L., Davis, A.S., Lynch, W.G., MacKenzie, I., Palethorpe, S., Siegl, P.K., Strang, I., Sullivan, A.T., Wallis, R., Camm, A.J., Hammond, T.G., 2003. Cardiovasc. Res. 58 (1), 32–45.
Robertson, C., Tran, D.D., George, S.C., 2013. Stem Cells 31 (5), 829–837.
Shi, L., Rong, X., Wang, Y., Ding, S., Tang, W., 2018. Biosens. Bioelectron. 102, 41–48.
Shi, L., Wang, Y., Chu, Z., Yin, Y., Jiang, D., Luo, J., Ding, S., Jin, W., 2017. J. Mater. Chem. B 5 (5), 1073–1080.
Takasuna, K., Asakura, K., Araki, S., Ando, H., Kazusa, K., Kitaguchi, T., Kunimatsu, T., Suzuki, S., Miyamoto, N., 2017. J. Pharmacol. Toxicol. Methods 83, 42–54.
Thavandiran, N., Dubois, N., Mikryukov, A., Masse, S., Beca, B., Simmons, C.A., Deshpande, V.S., McGarry, J.P., Chen, C.S., Nanthakumar, K., Keller, G.M., Radisic, M., Zandstra, P.W., 2013. Proc. Natl. Acad. Sci. USA 49 (110), E4698–E4707. https://doi.org/10.1073/pnas.1311120110. PMID: 24255110.
Tiburcy, M., Didie, M., Boy, O., Christalla, P., Doker, S., Naito, H., Karikkineth, B.C., El-Armouche, A., Grimm, M., Nose, M., Eschenhagen, T., Zieseniss, A., Katschinksi, D.M., Hamdani, N., Linke, W.A., Yin, X., Mayr, M., Zimmermann, W.H., 2011. Circ. Res. 109 (10), 1105–1114.
Yamazaki, K., Hihara, T., Taniguchi, T., Kohmura, N., Yoshinaga, T., Ito, M., Sawada, K., 2012. Toxicol. Vitr.: Int. J. Publ. Assoc. BIBRA 26 (2), 335–342.
Yang, X., Pabon, L., Murry, C.E., 2014. Circ. Res. 114 (3), 511–523.
Zhang, D., Shadrin, I.Y., Lam, J., Xian, H.Q., Snodgrass, H.R., Bursac, N., 2013. Biomaterials 34 (23), 5813–5820.
Zhang, B.Y., Green, J.V., Murthy, S.K., Radisic, M., 2012a. PLoS One 7 (5).
Zhang, J., Klos, M., Wilson, G.F., Herman, A.M., Lian, X., Raval, K.K., Barron, M.R., Hou, L., Soerens, A.G., Yu, J., Palecek, S.P., Lyons, G.E., Thomson, J.A., Herron, T.J., Jalife, J., Kamp, T.J., 2012b. Circ. Res. 111 (9), 1125–1136.
Zhang, J., Wilson, G.F., Soerens, A.G., Koonce, C.H., Yu, J., Palecek, S.P., Thomson, J.A., Kamp, T.J., 2009. Circ. Res. 104 (4), e30–e41.
Zhang, N., Stauffer, F., Simona, B.R., Zhang, F., Zhang, Z.M., Huang, N.P., Voros, J., 2018. Biosens. Bioelectron. 112, 149–155.